Chemie der Erde 77 (2017) 503–515

Contents lists available at ScienceDirect

Chemie der Erde

journal homepage: www.elsevier.de/chemer

Rutile geochemistry and thermometry of eclogites and associated garnet-mica schists in the Biga Peninsula, NW Turkey

Firat Şengün [a,*], Thomas Zack [b], Gültekin Topuz [c]

[a] Çanakkale Onsekiz Mart University, Terzioğlu Campus, Faculty of Engineering, Department of Geological Engineering, 17100, Çanakkale, Turkey
[b] University of Gothenburg, Department of Earth Sciences, Box 460, 40530, Gothenburg, Sweden
[c] Istanbul Technical University, Eurasia Institute of Earth Sciences, 34469, Istanbul, Turkey

ARTICLE INFO

Article history:
Received 9 February 2017
Received in revised form 29 May 2017
Accepted 2 July 2017
Editorial handling - Astrid Holzheid

Keywords:
Rutile
Source-rock lithology
Zr-in-rutile
High-pressure
NW Turkey

ABSTRACT

In northwest Turkey, high-pressure metamorphic rocks occur as exotic blocks within the Çetmi mélange located on the south of the Biga Peninsula. Rutile chemistry and rutile thermometry obtained from the eclogite and associated garnet-mica schist in the Çetmi mélange indicate significant trace element behaviour of subducted oceanic crust and source-rock lithology of detrital rutiles. Cr and Nb contents in detrital rutile from garnet-mica schist vary from 355 to 1026 µg/g and 323 and 3319 µg/g, respectively. According to the Cr-Nb discrimination diagram, the results show that 85% of the detrital rutiles derived from metapelitic and 15% from metamafic rocks. Temperatures calculated for detrital rutiles and rutiles in eclogite range from 540 °C to 624 °C with an average of 586 °C and 611 °C to 659 °C with an average of 630 °C at P = 2.3 GPa, respectively. The calculated formation temperatures suggest that detrital rutiles are derived from amphibolite- and eclogite-facies metamorphic rocks. Amphibolite-facies rocks of the Kazdağ Massif could be the primary source rocks for the rutiles in the garnet-mica schist from the Çetmi mélange. Nb/Ta ratios of metapelitic and metamafic rutiles fall between 7–24 and 11–25, respectively. Nb/Ta characteristics in detrital rutiles may reflect a change in source-rock lithology. However, Nb/Ta ratios of rutiles in eclogite vary from 9 to 22. The rutile grains from eclogites are dominated by subchondritic Nb/Ta ratios. It can be noted that subchondritic Nb/Ta may record rutile growth from local sinks of aqueous fluids from metamorphic dehydration.

© 2017 Elsevier GmbH. All rights reserved.

1. Introduction

Rutile is a robust accessory mineral that has attracted considerable attention in the last decade as a petrogenetic indicator (e.g., Zack et al., 2004; Triebold et al., 2007; Luvizotto et al., 2009; Meinhold, 2010). The widespread occurrence of rutile in a large range of lithologies (Force, 1980) and its high physical and chemical stability during erosion, weathering, transport and diagenesis make rutile one of the most stable heavy minerals (e.g., Morton and Hallsworth, 1999). Trace element composition of rutile has been recently used as a tool for provenance studies (Zack et al., 2004; Stendal et al., 2006; Triebold et al., 2007; Meinhold et al., 2008; Morton and Chenery, 2009; Okay et al., 2011; Liu et al., 2014). Rutile potentially provides significant information about source-rock lithology and metamorphic grade in high-pressure metasedimentary rocks (Zack et al., 2002; 2004; Meinhold et al., 2008; Morton and Chenery, 2009). Rutiles can be separated into metapelitic and metamafic origin in provenance studies based on the Cr-Nb discrimination diagram.

Rutile is a major titanium-bearing phase that carries the high field strength elements (HFSE) and dominates the Nb, Ta and Ti budgets of high-pressure metamorphic rocks in subduction zone systems (Brenan et al., 1994; Green, 1995; Foley at al., 2000; Rudnick et al., 2000; Ding et al., 2013). Nb/Ta ratios of rutile have been used as tracer of geochemical processes of the crust-mantle differentiation through subduction zone metamorphism, magma evolution and element cycling (e.g., Saunders et al., 1980; Münker, 1998; Klemme et al., 2005; Schmidt et al., 2008; Ding et al., 2009), as all the known mantle and crustal reservoirs have primarily subchondritic Nb/Ta and Zr/Hf ratios (e.g., Green, 1995; Foley et al., 2000; Rudnick et al., 2000; Zack et al., 2002; Ding et al., 2009). Rutile has become an important tool for evaluating metamorphic temperatures, especially in eclogite- and granulite-facies rocks (e.g., Zack et al., 2002; Spear et al., 2006; Luvizotto et al., 2009; Ewing et al., 2013; Gao et al., 2014; Liu et al., 2014) with the calibration of Zr-in-rutile thermometers (Zack et al., 2004; Watson et al., 2006; Tomkins et al., 2007).

* Corresponding author.
E-mail address: firatsengun@comu.edu.tr (F. Şengün).

http://dx.doi.org/10.1016/j.chemer.2017.07.001
0009-2819/© 2017 Elsevier GmbH. All rights reserved.

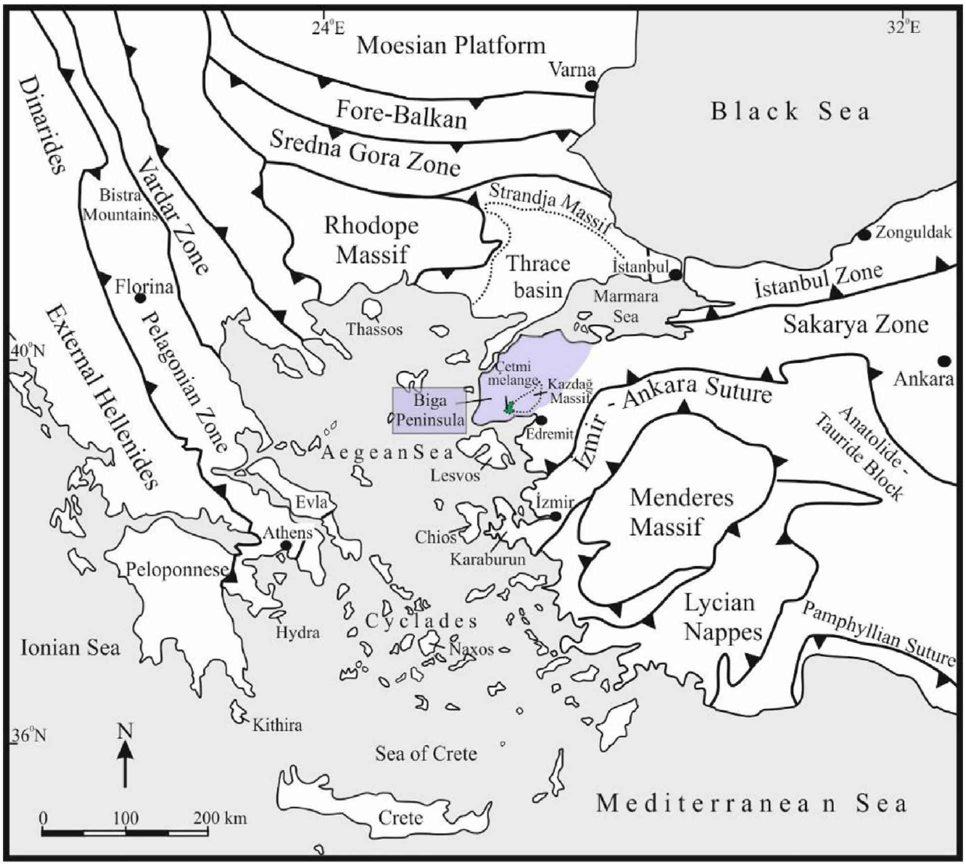

Fig. 1. Simplified tectonic map of the Eastern Mediterranean region indicating the major geotectonic units and the bounding sutures (modified from Meinhold et al., 2010; Okay et al., 2006).

In this study, the geochemical parameters of rutile in HP rocks from the Biga Peninsula have been investigated. This study focuses on the trace element composition of rutiles and Zr-in-rutile thermometry of eclogites and associated garnet-mica schist from the Biga Peninsula in the northwest of Turkey (Fig. 1). The purpose of this study is to provide first insights into the source-rock lithology of detrital rutiles in HP metasedimentary rocks in the Çetmi mélange and trace element behaviour of subducted oceanic crust, since the source-rock lithology of detrital rutiles is missing in NW Turkey and it is crucial for paleogeographic construction of NW Turkey. Trace element geochemistry was used to distinguish rutile derived from metapelitic and metamafic rocks by using Nb-Cr discrimination diagram. Zr-in-rutile geothermometry was applied to calculate metamorphic temperatures.

2. Geologic framework

The Biga Peninsula forms the northwest extremity of Turkey. It is bordered to the north by the Strandja Massif and the Thrace Basin, and the Aegean Sea marks the western and southern borders (Fig. 1). The Biga Peninsula in NW Turkey is dominated by the widespread occurrences of Tertiary plutonic and associated volcanic rocks. This magmatism is post-collisional with respect to the continental amalgamation along the İzmir-Ankara suture zone, and lies in a back-arc position with respect to the present-day subduction front along the Crete. (e.g., Borsi et al., 1972; Okay and Satır, 2000b; Okay et al., 2001). Apart from these magmatic rocks, the Biga Peninsula includes the following main rock associations: (1) amphibolite-facies basement rocks of the Kazdağ Massif (Carboniferous; Okay and Satır, 2000b; Duru et al., 2004; Yaltırak and Okay, 2004; Cavazza et al., 2009; Şengün and Zack, 2016a), and greenschist-facies rocks of the Çamlıca metamorphic unit (Late Cretaceous; Okay and Satır, 2000a; Şengün et al., 2011), and Karabiga metamorphic unit (Late Cretaceous; Beccaletto et al., 2007; Aygül et al., 2012); (2) the Triassic-Early Jurassic units of the Karakaya Complex exposed only in the eastern part of the Biga Peninsula (Okay and Göncüoğlu, 2004); (3) the subduction-accretion Çetmi mélange (mid-Cretaceous; Okay et al., 1990; Beccaletto et al., 2005); and (4) the Permo-Triassic Karadağ metamorphic unit that is tectonically overlain by the Lower Cretaceous Denizgören ophiolite (Okay et al., 1990; Beccaletto and Jenny, 2004). All of the units are unconformably covered by the Tertiary sedimentary units (Fig. 2a).

Two exotic blocks of eclogite-garnet mica schist occur within the Çetmi mélange in the southern part of the Biga Peninsula (Fig. 2b). These HP blocks are about 2–4 km long and less than 1 km wide. The Çetmi mélange is mainly composed of spilitized mafic volcanic rocks, blocks of Upper Triassic neritic and pelagic limestones, greywacke-shale matrix, minor radiolarian chert and serpentinite/listvenite slices (Beccaletto, 2004; Beccaletto et al., 2005) and are unmetamorphosed. The Çetmi melange is unconformably overlain by various types of Neogene sedimentary and volcanic rocks. Rb-Sr phengite ages from two eclogite samples within the Çetmi mélange yielded a mid-Cretaceous age of 100 Ma, which is interpreted as a cooling age (Okay and Satır, 2000b). This mid-Cretaceous age sets the upper time limit for deposition of the protolith of the metasedimentary rocks.

3. Petrography

A total of 7 high-pressure rock samples were chosen for rutile chemical analyses. Of these, four samples 1533 (35S 0463412N-4381876E), 1544 (35S 0461682N-4381659E), 1549 (35S

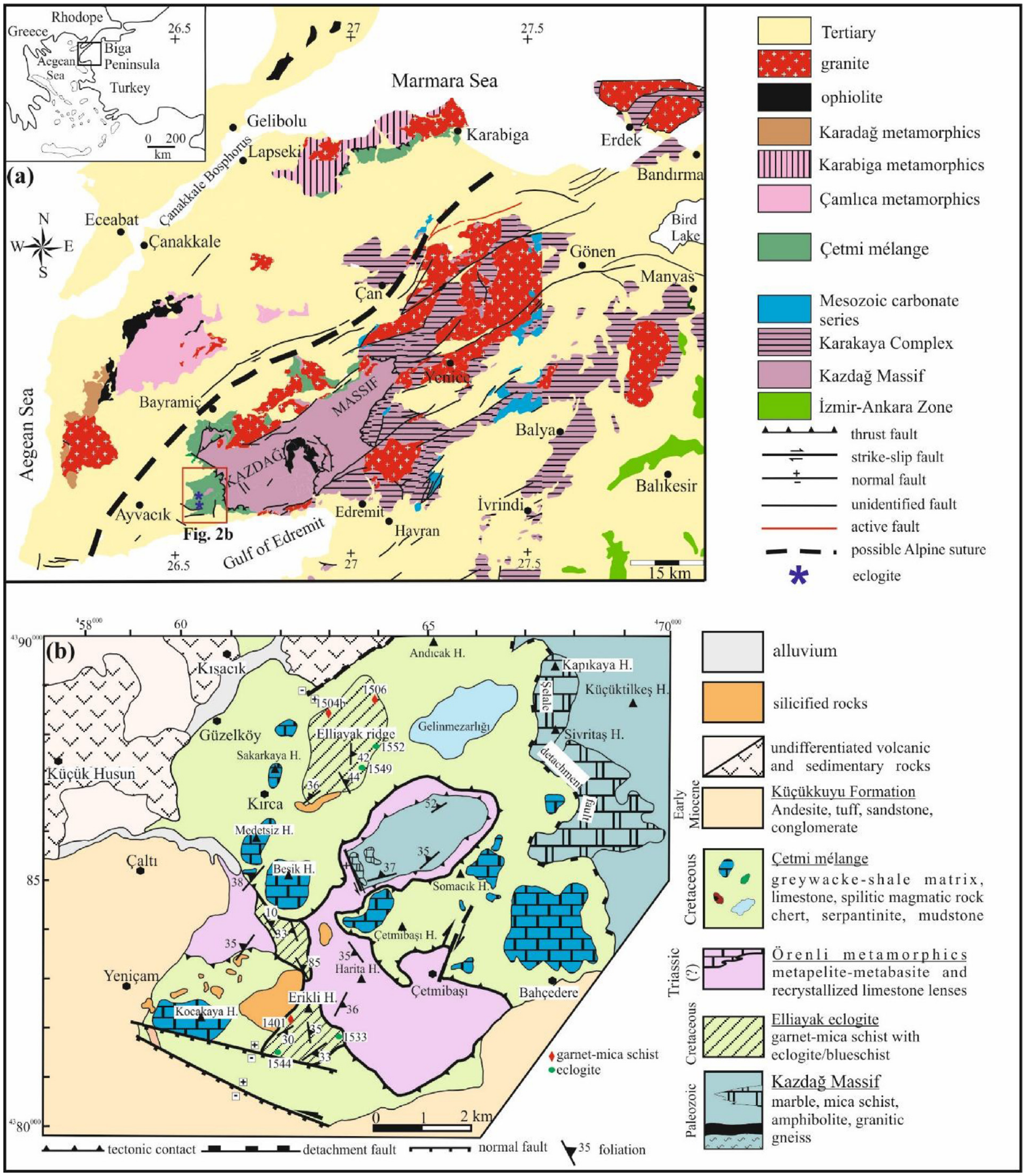

Fig. 2. (a) Generalized geological map of the Biga Peninsula (modified from MTA, 2012). Inset map shows location of the Biga Peninsula. (b) Detailed geological map of the Çetmi mélange (modified from Tunç, 2008).

0463457N-4387258E) and 1552 (35S 0463910N-4387808E) come from eclogites and three samples 1401 (35S 0462072N-4382365E), 1504b (35S 0462948N/4388636E) and 1506 (35S 0463912N-4388545E) come from garnet-mica schist. Sample locations are shown in Fig. 2b. The garnet-mica schist forms well foliated coarse-grained, silvery grey homogenous rocks with eclogite horizons. The foliation in the garnet-mica schist is parallel to the elongation axis of eclogite slices. The garnet-mica schist is mainly composed of garnet + quartz + phengite + paragonite (Fig. 3a). Rutile, titanite and zircon form the accessory minerals. The size of the garnets is macroscopically ranging between 0.4 and 0.8 cm. Euhedral garnet porphyroblasts include quartz and phengite inclusions. Syntectonic garnet porphyroblasts occur in garnet-mica schist (Fig. 3b). Detrital rutile grains do not show the presence of inclusions (Fig. 3c) and are 60–80 μm in diameter in their longest dimension and occur as separate grains in the matrix. The morphology of rutile is typical for detritic origin and grains are mostly dark brown, subrounded to rounded and elongated with some pristine euhedral shapes. Several grains are separated along the main cleavage direction and have a stubby appearance. Some rutile grains have a thin ilmenite overgrowth and retrograde rim of titanite. Small zircons (<20 μm) are present either in garnet or the matrix.

The eclogites are coarse grained, greenish, massive and banded rocks. The high-pressure assemblages in eclogite consist

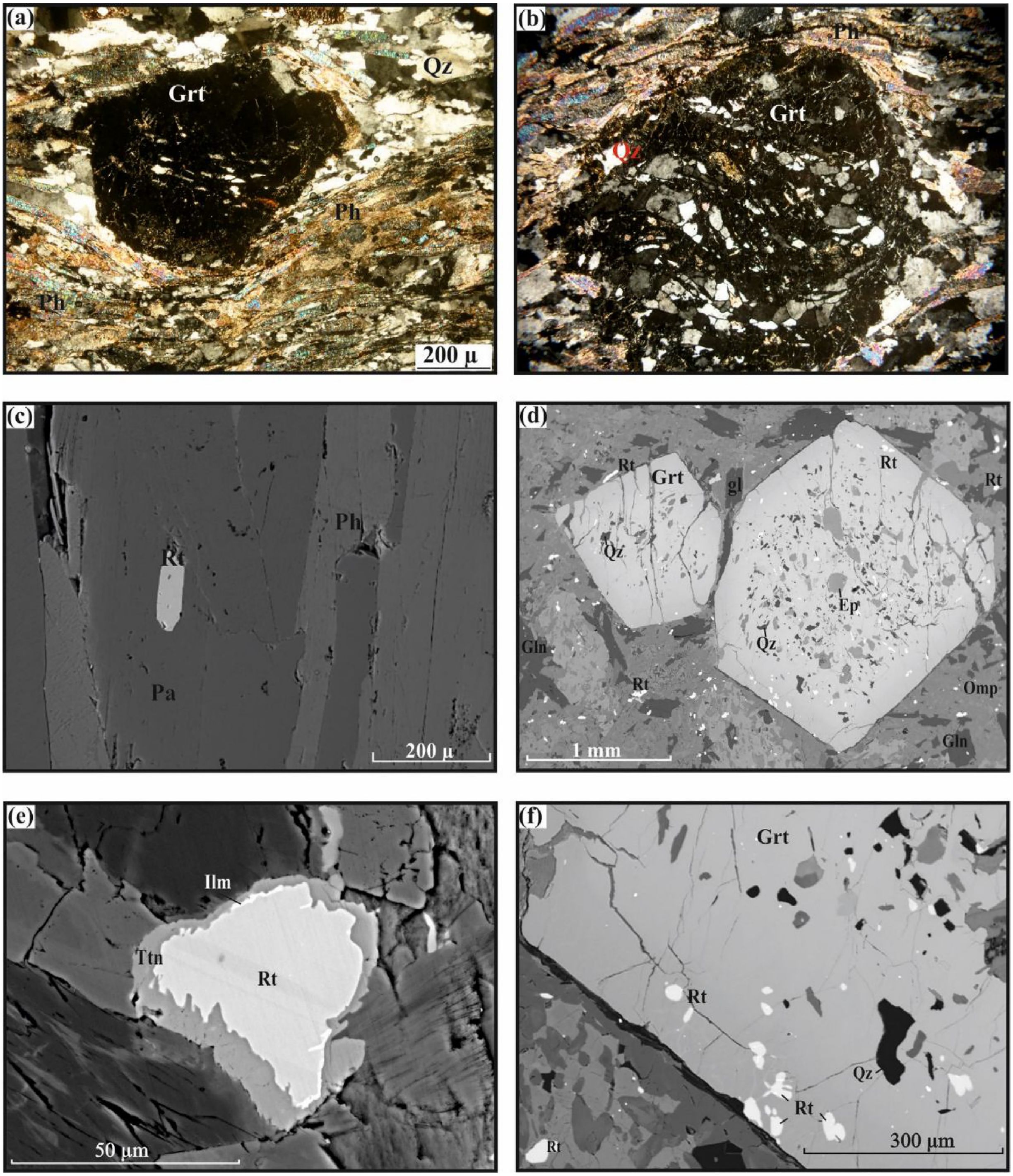

Fig. 3. (a) Microphotograph of the high-pressure garnet-mica schist. (b) Syntectonic garnet porphyroblast in the garnet-mica schist. (c) BSE image of rutile grain occurring in the garnet-mica schist. (d) BSE image of typical eclogite paragenesis with garnet, omphacite, glaucophane. (e) BSE image of rutile grain surrounded by titanite and with thin ilmenite overgrowth. (f) BSE image of garnet porphyroblasts comprising glaucophane, epidote, quartz and rutile inclusions.

of omphacite + garnet + epidote + glaucophane + quartz + phengite (Fig. 3d). Typical accessory minerals are rutile, zircon and titanite. Euhedral, relatively large (0.2–0.8 cm) porphyroblasts of garnet, are scattered through a fine-grained matrix, and contain inclusions of mainly quartz, epidote, phengite, glaucophane, Ca-amphibole and rutile. Omphacite is fine grained and forms up to 2 mm long crystals in the matrix. Rutile grains occur in the matrix and as inclusions in garnet (Fig. 3e, f). Sodic amphibole in eclogite is glaucophane in composition, and is typically fine-grained and aligned with omphacite in the matrix. Glaucophane crystals are rimmed and partially replaced by Ca-amphibole. Glaucophane inclusions in garnet also show that glaucophane was present as a matrix phase in the eclogite stage. Rutile grains are mantled by titanite and thin ilmenite overgrowth (Fig. 3e). Ca-amphibole and chlorite occur in eclogite as secondary phases that are not in equilibrium with the high-pressure phases. The eclogite shows a greenschist-facies overprint with the replacement of garnet by chlorite, and titanite rims around rutile. The occurrences of chlorite in the garnet-mica schist also demonstrate the retrogradation at greenschist facies conditions.

4. Analytical methods

4.1. Sample preparation

Samples were prepared for trace element analysis as polished thin sections of 50 μm. Photomicrographs were taken to identify the exact spots for laser ablation analysis and prepared for orientation using reflected light in the laser ablation sample cell. Backscattered electron (BSE) images were obtained using a Hitachi S-3400N scanning electron microscope (SEM) at the University of Gothenburg to identify inclusions in rutile and document the most suitable spots for analysis. The operation conditions during the BSE imaging were maintained at 20 kV and 6.04 nA. Samples were cleaned by polishing with 1 μm alumina oxide powder to remove any carbon coating residual from SEM analysis. Then samples were put in an ultrasonic cleaning bath for 5 min and dried with ethanol-soaked tissue wiper to remove remaining surface contamination prior to being loaded into the laser ablation sample chamber.

4.2. LA-ICPMS analysis

The in-situ trace element analyses (Zr, Nb, Cr, Fe, Ta, Hf, V, W) of rutile were performed on prepared thick sections at the Department of Earth Sciences at the University of Gothenburg. All samples were analysed using New Wave NWR 213 laser ablation system coupled to an Agilent 8800 triple quadropole ICP-MS. A He-Ar mixture was used as carrier gas. Helium gas, which carries the laser ablated sample aerosol from the sample cell, is mixed with argon carrier gas and nitrogen as additional di-atomic gas to enhance sensitivity, and finally flows into the ICPMS torch. Helium is flushed through the ablation cup at ~1 ml/min. The helium reduces surface deposition during ablation, which increases sensitivity and also reduces fractionation owing to particle size bias (Eggins et al., 1998).

Trace elements in rutile were analysed using laser beam with a diameter of 30 μm at laser energy of ~6.2 J/cm^2 with a pulse repetition rate of 10 Hz. Each twelve unknown spots were bracketed by two analyses of the R10 rutile standard and two analyses of NIST SRM 610 glass standard. Signals were recorded over 60 s for each spot. The first 20 s were used to acquire background subtraction during laser warm-up. The following 30 s of dwell time were used for analysis of the sample by the ablation of rutile. The last 10 s were used for wash out. ^{51}V, ^{53}Cr, ^{57}Fe, ^{178}Hf, ^{181}Ta, ^{182}W, ^{232}Th (10 ms dwell time), ^{49}Ti, ^{93}Nb (5 ms dwell time) and ^{90}Zr, ^{238}U (30 ms dwell time) were analysed for trace element concentration in rutile. Titanium measured as ^{49}Ti was used as an internal standard element for all analyses. ^{90}Zr was used to determine the Zr concentration of rutile. The glass reference material NIST SRM 610 (Jochum and Nehring, 2006) and R10 (Luvizotto et al., 2009) rutile were used for external calibrations. The concentrations of elements were determined using "GLITTER version 4.4.4" software program (On-line interactive data reduction for LA-ICPMS microprobe (Van Achterbergh et al., 2000) on the basis of measurements of the following isotopes (mean detection limits given in brackets; 99% confidence interval): ^{49}Ti (0.1238 μg/g), ^{51}V (0.1528 μg/g), ^{53}Cr (0.5432 μg/g), ^{57}Fe (1.3184 μg/g), ^{90}Zr (0.0038 μg/g), ^{93}Nb (0.0077 μg/g), ^{178}Hf (0.0053 μg/g), ^{181}Ta (0.0039 μg/g), ^{182}W (0.0195 μg/g), ^{232}Th (0.0032 μg/g), and ^{238}U (0.0025 μg/g). Titanium content during data reduction was initially assumed to be 99 wt% TiO_2.

Rutile grains devoid of cracks and inclusions were chosen for spot analyses. Multiple analyses of selected grains were also performed to reveal the chemical homogeneity. The rutile grains from all samples were geochemically discriminated into those from metapelitic and metamafic according to their Cr and Nb contents. The temperature of each rutile was calculated by applying the Zr-in-rutile geothermometer of Tomkins et al. (2007) which takes into account the pressure effect on the uptake of Zr in rutile. The peak P-T conditions of the high-pressure metamorphic rocks in the Çetmi mélange were determined as 624 ± 17 °C and 2.26 ± 0.16 GPa based on TitaniQ geothermobarometry (Şengün and Zack, 2016b). Thus, the pressure was considered as ~2.3 GPa in the equation of Tomkins et al. (2007).

5. Results

5.1. Major and trace element compositions of high-pressure rocks

Eclogite and associated garnet-mica schist were analysed for major and trace element compositions. The results are given in Supplementary Material 1. Eclogites are characterized by low SiO_2 (47.2–48.8 wt.%), high TiO_2 (1.54–2.08 wt.%), $K_2O + Na_2O$ (2.61–3.47 wt.%, $Na_2O > K_2O$) contents and high Cr (130–360 μg/g), Nb (3.8–11.5 μg/g) contents (Şengün et al., 2012). The chondrite-normalized diagram for eclogite samples show flat REE patterns characteristic for enriched MORB (Fig. S1a).

Garnet-mica schists cover a SiO_2 range from 60.9 to 68.3 wt.%. Most garnet-mica schists have TiO_2 contents lower than 1%, which is lower than eclogites. Garnet-mica schists also show large ranges in Al_2O_3 of 11.1-15.6 wt.% and K_2O of 1.69-2.48 wt.%. The chondrite-normalized diagram for garnet-mica schist indicates the typical pattern of the Upper Continental Crust (UCC) with a strong enrichment in the LREE and a marked negative anomaly in Eu (Fig. S1b).

5.2. Rutile geochemistry

In total, 111 rutile grains from both garnet-mica schist and eclogite in the Çetmi mélange were analysed by LA-ICPMS and the results are listed in Tables 1 and 2, respectively. 63 detrital rutile grains come from three garnet-mica schists (1401, 1504b, 1506) and 48 rutile grains come from four eclogite samples (1533, 1544, 1549, 1552). In all samples, the rutiles vary in colour from yellowish to reddish brown. Rutile occurs as two different textural types in the studied samples. It occurs as single grains in the matrix between rock-forming minerals and as inclusion in garnet. The grain size of detrital matrix rutile in garnet-mica schist is mostly between 50 and 150 μm with an average of about 100 μm. Inclusion rutile has the grain size of about 20–30 μm. Matrix rutile in eclogite samples has a grain size between 60 and 80 μm. Rutile occurs as an inclusion in garnet (grain size of rutile: <20 μm). The different textural rutile types in eclogites and garnet-mica schist with the associated range of Zr concentrations and temperatures are summarized in Table 3 and Fig. 6.

Cr contents in detrital rutiles from garnet-mica schist vary from 355 to 1026 μg/g with an average of 618 μg/g. Nb concentrations have a large spread (Nb: 323–3319 μg/g with an average of 1141 μg/g). Cr and Nb contents of rutiles occuring in matrix range from 365 to 1026 μg/g (average 631 μg/g) and 323–2052 μg/g (average 1007 μg/g), respectively (Table 1, Fig. 4). Ta contents in matrix rutiles vary between 14 and 183 μg/g. Zr and Hf concentrations of rutiles range from 24 to 74 μg/g and 1 and 3 μg/g, respectively. However, inclusion rutiles in garnet have Cr concentration of 355–820 μg/g (average 580 μg/g) and Nb concentrations of 807–3319 μg/g (average 1537 μg/g). Ta concentrations of inclusion rutiles in garnet vary from 61 to 210 μg/g. Zr and Hf contents have little variation (Zr: 49–89 μg/g; Hf: 2–4). The high Fe contents (>1000 μg/g) of detrital rutile grains possibly give a hint at metamorphic origin, whereas magmatic rutile generally includes <1000 μg/g Fe (Zack et al., 2004).

There is also large variation in the trace element composition of rutile in eclogite samples. Cr and Nb concentrations in eclog-

Table 1
Trace element concentrations (μg/g) and the calculated temperature (°C) in rutile from the garnet-mica schist.

Element Sample no	Grain	V	Cr	Fe	Zr	Hf	W	Nb	Ta	U	Zr/Hf	Nb/Ta	Log (Cr/Nb)	T 2.3 GPa
1401	1	1270	457	4616	34	2	96	835	46	1.03	17	18	−0.26	560
	2	452	571	5191	89	3	49	3319	210	0.62	30	16	−0.76	621
	3	558	390	4095	66	2	34	1870	87	1.16	33	21	−0.68	601
	5	1165	626	4373	54	2	47	1031	66	1.45	27	16	−0.22	588
	7–1	369	680	3867	32	2	40	888	52	1.93	16	17	−0.12	557
	7–2	846	841	2036	39	2	32	948	88	0.23	20	11	−0.05	568
	8	462	877	3457	46	2	33	980	53	0.86	23	18	−0.05	578
	9	392	924	3875	44	2	41	1058	58	1.12	22	18	−0.06	575
	10	794	735	1984	35	2	25	917	50	0.22	18	18	−0.10	561
	11	1057	759	4256	63	3	68	1245	66	1.08	21	19	−0.21	598
	12	677	642	3068	54	3	139	1052	61	0.18	18	17	−0.21	588
	14–1	588	404	2368	37	2	35	947	78	0.18	19	12	−0.37	565
	14–2	657	399	2564	35	2	40	1030	76	0.25	18	14	−0.41	561
	16	812	547	2018	49	2	32	931	64	0.12	25	15	−0.23	582
1504b	1	1150	553	4360	89	4	160	1958	152	0.20	22	13	−0.55	621
	3	892	586	3395	64	3	125	2052	140	0.24	21	15	−0.54	599
	8	876	508	2905	85	4	158	2116	161	0.13	21	13	−0.62	618
	9	570	436	4159	73	3	140	2046	145	0.32	24	14	−0.67	612
	16	407	640	4884	62	3	106	1816	134	2.59	21	14	−0.45	601
	18	958	519	2607	87	4	150	1827	144	0.18	22	13	−0.55	624
	19	859	574	3719	82	4	138	1641	139	0.16	21	12	−0.46	620
	21	903	355	3829	74	3	164	807	124	0.00	25	7	−0.36	614
	22	576	487	3267	62	3	79	1674	155	0.34	21	11	−0.54	601
	23	362	543	3452	56	2	100	1879	178	0.46	28	11	−0.54	595
	24	473	647	4238	84	4	124	980	144	0.33	21	7	−0.18	622
	25	886	825	3169	55	2	132	1560	158	0.24	28	10	−0.28	594
	26	1260	558	4583	63	3	115	877	127	0.78	21	7	−0.20	603
	29	1014	584	2894	72	3	103	1689	183	0.66	24	9	−0.46	611
	30	937	817	2296	81	4	122	1077	137	0.23	20	8	−0.12	619
	31	906	878	3210	73	3	180	1212	144	0.00	24	8	−0.14	612
	32	452	520	3440	76	3	144	1478	138	0.43	25	11	−0.45	615
	35	485	687	4267	69	3	108	980	122	0.34	23	8	−0.15	609
	37	918	675	3868	72	3	138	878	126	0.26	24	7	−0.11	611
	38	549	820	3190	80	4	135	1207	162	0.41	20	7	−0.17	618
1506	5–1	772	483	2427	27	2	434	1066	48	0.25	13	22	−0.34	546
	5–2	1054	567	1970	64	3	446	464	41	0.37	21	11	0.09	599
	7	898	673	3926	43	2	396	850	76	0.42	21	11	−0.10	573
	10	864	1026	3921	37	2	269	1396	104	0.24	18	13	−0.13	564
	11–1	1177	945	2790	44	2	583	1048	52	0.57	22	20	−0.05	576
	11–2	716	625	2330	36	3	592	901	44	0.17	12	21	−0.16	564
	12–1	905	511	2918	53	2	412	832	51	0.41	27	16	−0.21	587
	12–2	407	602	6101	62	3	427	982	61	0.20	21	16	−0.21	598
	13	334	682	4092	30	2	486	884	45	2.09	15	20	−0.11	552
	14	923	505	3276	28	2	408	1060	56	0.45	14	19	−0.32	548
	16	976	365	2235	26	1	295	880	58	0.52	26	15	−0.38	545
	17	1110	537	2425	58	2	274	439	21	0.20	29	21	0.09	593
	18	1089	804	2062	40	2	539	902	60	0.17	20	15	−0.05	570
	19–1	1078	701	2400	26	1	445	961	72	0.19	26	13	−0.14	545
	19–2	986	722	2181	24	1	471	800	65	0.16	24	12	−0.04	540
	20	684	769	2308	52	2	585	918	46	0.33	26	20	−0.08	585
	21	691	566	2311	48	2	413	1116	46	0.23	24	24	−0.30	581
	22–1	1048	560	2444	26	1	432	1082	66	0.56	26	16	−0.29	545
	22–2	1027	532	4726	38	2	469	845	53	0.24	19	16	−0.20	567
	22–3	269	619	5866	33	2	445	840	57	0.29	16	15	−0.13	558
	23	985	621	2318	45	2	296	916	41	0.19	22	22	−0.17	577
	25–1	1124	447	2420	39	2	434	1167	60	0.20	20	19	−0.42	568
	25–2	1240	565	2096	66	3	461	397	21	0.32	22	19	0.15	601
	26	917	631	3904	54	2	279	1061	64	0.16	27	17	−0.23	588
	30	886	538	2105	61	3	235	458	18	0.22	20	25	0.07	596
	31	983	618	1948	74	3	408	323	14	1.81	25	23	0.28	614
	32	842	424	3425	67	3	425	323	20	0.32	22	17	0.12	602
	34	959	767	1967	48	2	287	1098	52	0.16	24	21	−0.16	581
	35	914	494	2133	25	1	414	1080	58	0.16	25	19	−0.34	541

Temperatures were calculated according to the calibration of Tomkins et al. (2007) at 2.3 GPa.

ites are lower than those in garnet-mica schist and range from 269 to 1363 μg/g with an average of 572 μg/g and 63–444 μg/g with an average 206 μg/g, respectively (Table 2, Fig. 4). Cr contents of matrix rutile in eclogite vary between 269 and 973 μg/g (average 525 μg/g). Nb contents of matrix rutile vary from 77 to 444 μg/g (average 218 μg/g). Ta contents range between 6 and 29 μg/g. Zr and Hf contents of matrix rutiles have higher than detrital rutiles in garnet-mica schist and vary from 79 to 150 μg/g and 3–7 μg/g. However, Cr and Nb concentrations of inclusion rutiles in garnet range from 379 to 1363 μg/g (average 628 μg/g) and 63–409 μg/g (average 193 μg/g), respectively. Ta contents of inclusion rutiles have large variations (3–27 μg/g). Zr and Hf concentrations range

Table 2
Trace element composition (μg/g) and the calculated temperature (°C) in rutiles from eclogites.

Element Sample no	Grain	V	Cr	Fe	W	Zr	Nb	Hf	Ta	Nb/Ta	Zr/Hf	Log (Cr/Nb)	T 2.3 GPa
1533	9	793	269	1485	1	131	210	7	13	16	19	0.11	649
	16	1641	400	3209	27	98	114	5	8	14	21	0.54	628
	17	1632	417	1871	44	120	113	6	7	15	20	0.57	642
	18	1681	379	4344	24	111	112	6	8	15	19	0.53	637
	19	1438	401	2272	21	85	117	4	8	15	24	0.54	619
	20	1480	423	2161	23	104	119	5	8	14	23	0.55	632
	21	2746	447	3411	18	121	119	6	9	14	22	0.57	643
1544	1	1189	379	7428	33	79	307	3	24	17	26	0.09	614
	10	1118	399	3459	37	90	361	3	21	17	27	0.04	622
	12	1121	395	3504	19	116	324	6	20	16	20	0.09	640
	13	1174	442	3630	30	89	308	3	19	16	32	0.16	622
	11	1047	592	4406	57	106	387	4	24	16	24	0.18	634
	3	1242	454	4580	27	129	347	6	21	16	20	0.12	648
	5–1	1118	525	4440	4	89	428	3	25	17	30	0.09	622
	5–2	1256	406	3680	23	106	381	4	23	16	27	0.03	634
	6	1254	424	3820	47	100	416	6	29	14	16	0.01	630
	15	1205	413	4730	36	77	345	3	23	15	26	0.08	611
	16	1188	455	5968	6	79	310	4	21	15	20	0.17	613
	17	1398	511	4787	71	78	409	4	27	15	22	0.10	612
	18	1229	468	3971	64	94	351	4	20	18	21	0.12	625
	19	1158	412	4554	63	85	370	4	25	15	23	0.05	618
	20	1186	549	4227	57	87	356	5	27	13	19	0.19	620
	21	1435	452	4383	78	76	401	4	21	19	20	0.05	611
	22	1153	446	3070	58	98	368	4	24	15	22	0.08	628
	24	1402	499	3556	100	100	444	3	26	17	33	0.05	630
	25	1170	552	2592	52	92	405	4	27	15	25	0.13	624
1549	5	1084	540	2869	1	106	85	4	6	14	27	0.80	634
	6	1182	891	2655	1	90	96	6	10	9	15	0.97	622
	7	1050	1044	2642	1	96	96	5	9	11	19	1.04	627
	8	1171	973	2885	2	86	87	4	8	11	24	1.05	619
	9	853	1363	3013	41	97	102	6	8	14	16	1.13	627
	10	923	1198	2954	14	92	90	5	3	22	18	1.13	624
	21	849	708	2525	69	87	92	5	9	11	17	0.89	620
	22	1022	541	3433	11	95	95	6	9	11	16	0.76	626
	23	889	879	2631	16	98	63	4	5	12	25	1.14	628
	24	868	882	2710	14	86	95	4	7	14	22	0.97	619
	25	843	803	3030	29	100	83	6	6	15	17	0.98	630
	26	900	876	2729	27	85	96	4	4	22	21	0.96	618
	27	813	834	3959	32	96	97	5	8	12	19	0.94	627
1552	10–1	1602	529	3709	24	150	77	7	6	13	20	0.84	659
	10–2	1241	299	3632	35	102	96	7	8	12	14	0.49	631
	4–1	1575	483	2788	63	120	87	6	6	15	19	0.75	643
	4–2	1592	452	2850	50	123	96	6	8	12	19	0.67	644
	8–1	1642	534	3382	37	109	97	6	7	14	17	0.74	635
	8–2	1560	552	3572	124	123	87	6	6	14	19	0.80	644
	7	1624	527	4005	23	134	82	7	5	15	21	0.81	651
	15	1647	499	4318	27	134	99	7	7	14	20	0.70	651
	16	1458	543	3621	44	127	90	6	7	12	22	0.78	646

Temperatures were calculated according to the calibration of Tomkins et al. (2007) at 2.3 GPa.

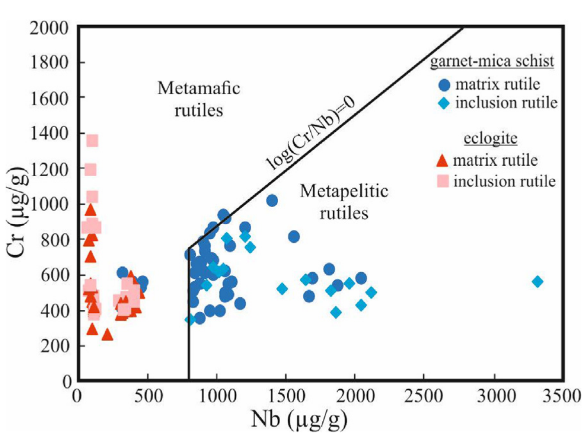

Fig. 4. Plot of Nb versus Cr contents of rutile grains for discrimination according to Meinhold et al. (2008).

from 77 to 134 μg/g and 3 and 7 μg/g. 63 detrital rutile grains from three garnet-mica schist and 48 rutile grains from eclogites are plotted for discrimination on the Cr-Nb diagram (Fig. 4). According to the Cr-Nb discrimination diagram, the results show that 85% of the detrital rutiles in garnet-mica schist derived from metapelitic and 15% from metamafic rocks.

All forty-seven matrix detrital rutile grains from garnet-mica schist show Nb/Ta ratios range from 7 to 24 with an average value of 15 (Fig. 5a). Nb/Ta ratios of sixteen inclusion rutile range between 7 and 21 with an average value of 13 (Fig. 5a). Rutile grains mostly have subchondritic Nb/Ta ratios (chondritic Nb/Ta = 19.9, Münker et al., 2003), whereas twelve rutiles in garnet-mica schist have superchondiritic Nb/Ta values ranging from 20 to 25 (Fig. 5b). All detrital rutile grains have subchondritic Zr/Hf ratios of 12–33 (Fig. 5b; chondritic Zr/Hf = 34.3, Münker et al., 2003).

Rutile grains from eclogites have relatively low Nb/Ta ratios (9–18, average 15), which are all subchondritic (Fig. 5b). Two grains have superchondritic Nb/Ta with an average of 22. All forty-eight

Table 3
Zr concentrations and temperatures in different positions of rutile grains.

	Eclogite								Garnet-mica schist			
Sample	1533		1544		1549		1552		1401		1504b	
	Zr (μg/g)	T(°C)	Zr (μg/g)	T(°C)	Zr (μg/g)	T(°C)	Zr (μg/g)	T(°C)	Zr (μg/g)	T(°C)	Zr (μg/g)	T(°C)
Rt in matrix	98	628	79	614	97	627	150	659	34	560	64	599
	120	642	90	622	92	624	102	631	32	557	62	597
	131	649	116	640	87	620	120	643	39	568	62	597
	121	643	89	622	86	619	123	644	46	578	56	591
			106	634	100	629	109	635	44	575	55	589
			129	648			123	644	35	561	63	598
			89	622					37	565	72	607
			106	634					35	561	73	608
			100	629							69	607
			100	629							72	607
			92	624								
Rt in garnet	111	637	77	611	106	634	134	651	89	621	89	621
	85	619	79	613	90	622	134	651	66	601	85	618
	104	632	78	612	96	627	127	646	54	588	73	608
			94	625	86	619			63	598	87	620
			85	618	95	626			54	588	82	616
			87	620	98	628			49	582	74	609
			76	611	85	618					84	617
			98	628	96	627					81	615
											76	611
											80	614

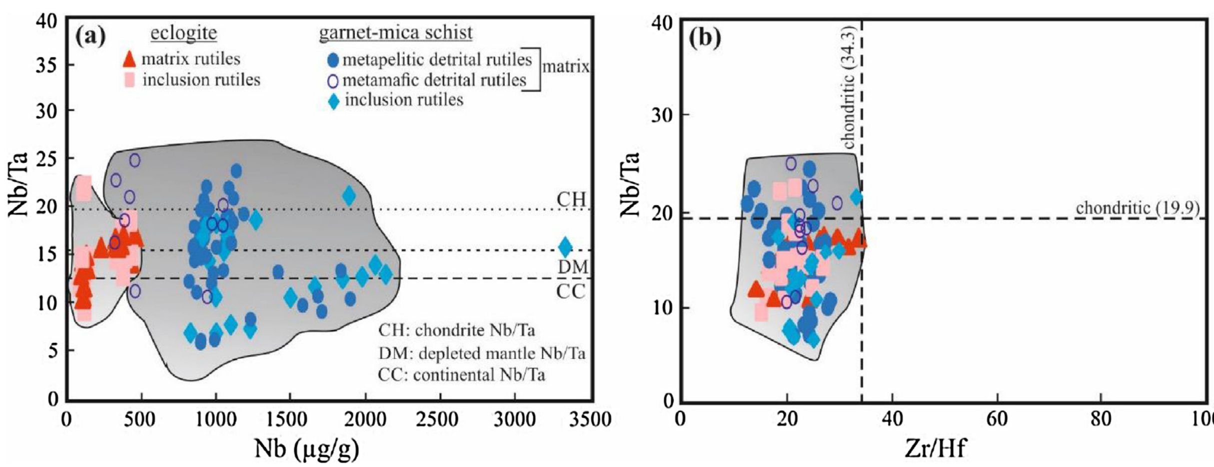

Fig. 5. Element ratio plots. Points represent individual analyses. (a) Nb versus Nb/Ta. (b) Zr/Hf versus Nb/Ta diagram. Generally Nb/Ta and Zr/Hf of rutile are subchondritic. Dashed lines refer to chondritic values for continental crust, depleted mantle, Nb/Ta and Zr/Hf (Barth et al., 2000; Münker et al., 2003).

rutile grains have subchondritic Zr/Hf (14–33) with an average of 21 compared to the chondritic Zr/Hf value of 34.3 (Fig. 5b; Münker et al., 2003).

5.3. *Zr-in-rutile thermometry*

Rutile grains from both garnet-mica schist and eclogites were analysed by LA-ICPMS for their Zr contents. The temperatures were calculated by using the pressure-dependant Zr-in-rutile thermometer of Tomkins et al. (2007). The results of Zr-in-rutile thermometry are shown in Fig. 6. Zr concentrations in the metapelitic detrital rutiles occuring in matrix of the garnet-mica schist range from 24 to 73 μg/g. Zr-in-rutile temperatures range from 540 °C and 612 °C with an average of 578 °C at P = 2.3 GPa for rutiles in garnet-mica schist. Metamafic detrital rutiles have higher Zr concentrations. Zr contents of metamafic rutiles vary between 39 and 74 μg/g. This corresponds to temperatures of 568 °C and 614 °C, which is identical to metapelitic rutiles. However, inclusion rutile grains in garnet have higher Zr contents than those occurring in matrix from garnet-mica schist (Zr: 54–89 μg/g), and correspond-

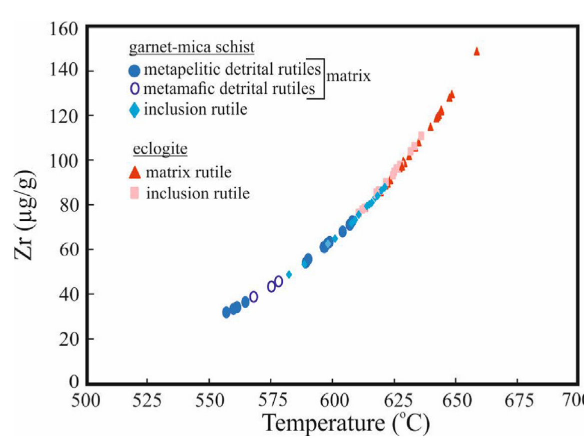

Fig. 6. Plot of calculated temperature range of the Zr-in-rutile thermometer versus Zr concentrations.

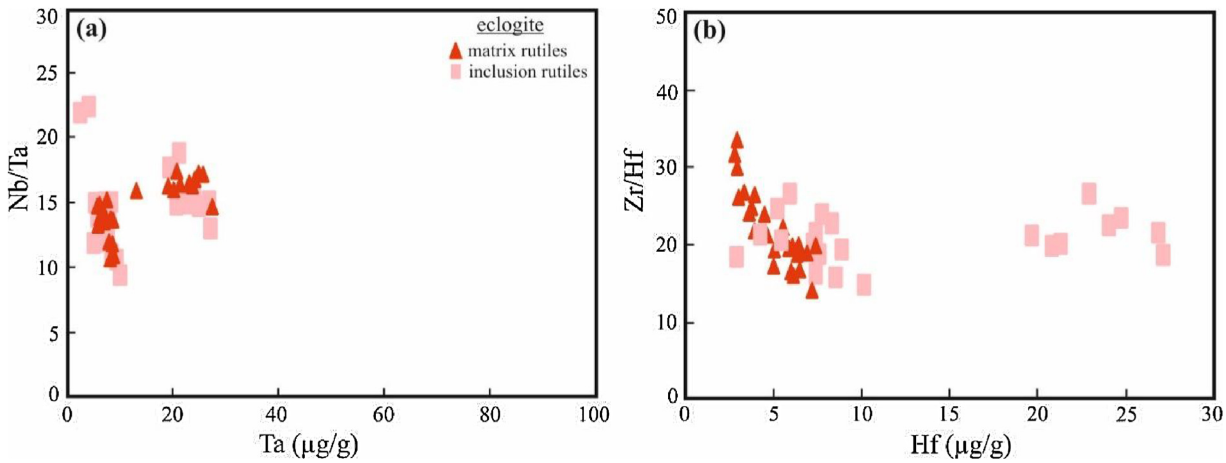

Fig. 7. Element ratio plots. Points represent individual analyses. (a) Ta versus Nb/Ta. (b) Hf versus Zr/Hf.

ing Zr-in-rutile temperatures range from 582 °C to 624 °C with an average of 610 °C (Fig. 6). The Zr distributions for the eclogite and associated garnet-mica schist are shown as histograms in Fig. S2.

Rutile grains in matrix from eclogites have high Zr concentrations and range from 79 to 150 µg/g. Zr-in-rutile thermometry for eclogites yielded matrix rutile formation temperatures of 614 °C and 659 °C with an average of 633 °C at P = 2.3 GPa. Zr contents of inclusion rutile grains in garnet vary from 76 to 134 µg/g. This corresponds to temperatures of 611 °C and 651 °C with an average of 626 °C (Fig. 6).

6. Discussion

6.1. Rutile geochemistry

A Cr-Nb discrimination diagram was used to determine the source rock lithology of the high-pressure metamorphic rocks exposed on the Çetmi mélange. Mafic and felsic source rock lithologies can be seperated by means of log (Cr/Nb). Positive log (Cr/Nb) values in rutile mostly exhibit a metamafic source whereas negative values suggest a derivation from metapelitic source (Triebold et al., 2007). It also would be significant to correlate such provenance indicator with temperature.

Using the Cr-Nb diagram, 63 detrital rutile grains from three garnet-mica schists and 48 rutile grains from eclogites are plotted for discrimination (Fig. 4). The results of rutile Cr-Nb systematics show a major input from metapelitic lithologies (85% of detrital rutile grains) and a minor input from metamafic lithologies (15% of detrital rutile grains) in garnet-mica schist. However, eclogites in the Çetmi mélange have compositions typical for derivation from metamafic rocks. The potential source of detrital rutile grains from garnet-mica schist with Cr<Nb and Nb>800 µg/g is derived from metapelitic rocks such as mica-schist and paragneisses, whereas rutile grains with Cr > Nb and those with Cr < Nb at Nb < 800 µg/g are suggested to be derived from mafic rocks such as eclogites and gabbros (Meinhold et al., 2008).

Nb and Ta would dominate the whole-rock Nb and Ta budget and the average Nb/Ta ratio of rutile may be identical to that of the bulk rock. Nb/Ta ratios in metamafic rutiles from garnet-mica schist have a relatively large range (11–25), which is slightly larger than metapelitic rutiles (7–24) (Fig. 5a). This may be accounted by differences in source-rock lithology. The metapelitic rutile grains have mostly subchondritic Nb/Ta ratios (7–24) with an average of 15 (Fig. 5b). Moreover, the metapelitic rutiles with suprachondritic Nb/Ta are more abundant than metamafic rutiles from garnet-mica schist samples. Moreover, inclusion rutiles in garnet have mostly subchondritic Nb/Ta ratios (7–21) with an average value of 13 except one inclusion rutile grain. In general, there is an overlap between Nb contents, Nb/Ta and Zr/Hf ratios in detrital rutiles and source-rock rutiles (Fig. 5a, b). Therefore, Nb/Ta, Zr/Hf ratios, Nb, Zr and Hf contents in detrital rutiles well reflect source rock compositions. Nb/Ta ratios of 6–40 in metapelitic and 12–30 in metamafic rutiles have been observed from Devonian-Carboniferous amphibolite-facies clastic rocks in the Istanbul Zone (Okay et al., 2011). Metapelitic and metamafic detrital rutiles from Bixiling in Central Dabie UHPM zone have also Nb/Ta ratios of 7.7-20.5 and 11–27.3, respectively (Liu et al., 2014). These ranges are comparable with our rutile grains in the Çetmi mélange.

The increase in Nb/Ta and Zr/Hf ratios in eclogites is mainly caused by a decrease in Ta and Hf contents (Fig. 7a, b). This suggests that differential incorporation of Nb and Ta into rutile during its growth is a basic cause for the Nb/Ta differentiation due to a significant difference in their mass. Accordingly, the increase in Nb/Ta ratios with the decreased Ta content can be attached to the effect of metamorphic dehydration at subduction zones on rutile Nb/Ta differentiation (Schmidt et al., 2009; Gao et al., 2014). Dehydration metamorphism is a common mechanism for rutile formation in subduction processes. Nb and Ta have the same oxidation state and similar ionic radii (Meinhold, 2010) and thus would remain tightly coupled during geochemical processes in the crust-mantle differentiation system. Rutile compositions in eclogites mostly display subchondritic Nb/Ta values (chondritic value 19.9, Münker et al., 2003) with a range of 9–22 and Zr/Hf values (chondritic value 34.3 ± 0.3, Münker et al., 2003) range between 14 and 33 (Fig. 5b). However, two inclusion rutile grains from sample 1549 have suprachondritic Nb/Ta values. It is probable that the subchondritic Nb/Ta ratios may record rutile growth from local sinks of aqueous fluids from metamorphic dehydration. Subchondritic Nb/Ta ratios occur in rutile from both medium to high-grade metamorphic regions (e.g., Meyer et al., 2011; Luvizotto and Zack, 2009; Ewing et al., 2013) and HP metamorphic regions (Xiao et al., 2006; John et al., 2011; Huang et al., 2012). In contrast, suprachondritic Nb/Ta ratios may suggest rutile growth from supercritical fluids or their products of phase separation into immiscible aqueous fluids and hydrous melts (Zheng et al., 2011).

6.2. Zr-in-rutile thermometry

The formation temperatures were calculated by the equations of Tomkins et al. (2007) with a pressure correction. The application of the Zr-in-rutile geothermometer of Tomkins et al. (2007) requires a pressure estimate for rutile growth.

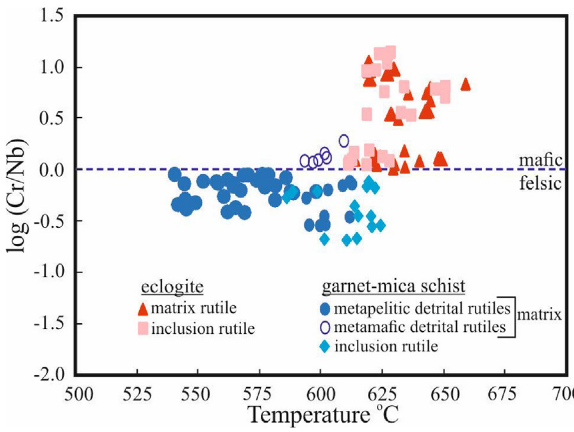

Fig. 8. Plot of temperatures calculated from Zr concentrations versus log (Cr/Nb). Mafic and felsic compositions according to log (Cr/Nb) are shown (Meinhold et al., 2008).

The calculated rutile temperatures for metapelitic detrital rutile grains in the garnet-mica schist range between 540 °C and 612 °C with an average of 578 °C at P = 2.3 GPa. Zr-in-rutile temperatures of inclusion rutiles in garnet range from 582 °C to 624 °C with an average of 610 °C, which is slightly higher than detrital matrix rutiles in garnet-mica schist (Fig. 6). This indicates that Zr-in-rutile temperatures can be readily changed after peak metamorphic conditions. However, the temperatures of inclusion rutiles in garnet-mica schist overlap to the temperatures of inclusion rutiles in eclogites. This suggests that these rutiles experienced similar metamorphic conditions (Fig. 6). The calculated temperatures for metapelitic rutiles are lower than the peak metamorphic temperature of 624 °C, which could be attributed to diffusion, recrystallization and interaction of rutiles with intensive retrograde fluid during exhumation (Chen and Li, 2008; Liu et al., 2014).

Detrital rutile grains with felsic compositions give usually lower maximum temperatures than rutile grains deriving from metamafic rocks (Fig. 8). The difference between both is smaller than 50 °C. However, some metapelitic rutiles and metamafic source indicate that source rocks overlap in their calculated formation temperatures. Such compatible temperatures not only show that detrital rutile grains truly reflect their provenance but also it demonstrates that high-pressure eclogites and their surrounding garnet-mica schist experienced similar metamorphic conditions together during the deep burial of these oceanic rocks.

Zr concentrations in metapelitic rutiles are systematically lower by 45–55 μg/g than metamafic rutiles in eclogite. Zr concentrations in rutile could be partly reduced by retrogression (Zack et al., 2004; Chen and Li, 2008), which explains the cause of lower Zr contents in metapelitic rutiles compared to metamafic rutiles. Detrital rutiles could also have grown from a different fluid at lower temperatures in their source rocks. Therefore, the difference in fluid composition can give rise to the difference in metamorphic temperature. Moreover, the Zr distribution in metamafic rutiles are more scattered than in metapelitic rutiles. This characteristic difference could be explained by the higher content of water in pelites versus mafic rocks (Hermann et al., 2006; Liu et al., 2014; Nichols et al., 1994; Schmidt et al., 2004). Thus, the Zr diffusivity in rutile is faster in metapelites than in the relative dry metamafic environment (Cherniak et al., 2007).

Rutile formation temperatures for metamafic rutile grains in eclogite vary from 611 °C and 659 °C with an average of 630 °C at P = 2.3 GPa. It is noted that both Zr contents and calculated temperatures of inclusion rutile and matrix rutile from three eclogite samples overlap to each other (Fig. 6). This suggests that all rutiles in eclogites occurring on the southern part of the Biga Peninsula experienced a similar metamorphic evolution. Moreover, rutile inclusion in garnet is probably to retain its original equilibrated Zr contents, given the very restricted ability to exchange Zr with the host phase during retrogression.

Eclogites and associated garnet mica schist experienced eclogite-facies metamorphism based on the Zr-in-rutile thermometry (Fig. 9). Fig. 9 indicates no input metapelitic rutile from greenschist- or blueschist-facies rocks. Amphibolite- and eclogite-facies lithologies are the most reasonable source rocks for this type of rutile.

6.3. *The source rock lithology of detrital rutile grains*

Eclogites have already been investigated for whole-rock major, trace and rare earth element (REE) contents (Şengün et al., 2012). The protolith of eclogite was an ocean-related magmatic rock as that of the garnet-mica schist was an associated sediment. The chondrite- and N-type MORB-normalized diagrams for eclogites indicate flat REE patterns characteristics for enriched MORB or OIB (ocean island basalt). The chondrite-normalized REE profiles for the garnet-mica schist show the typical pattern of the upper-continental crustal source with a strong enrichment in the light REE and negative Eu anomalies (Fig. S1). The protolith of the garnet-mica schist was possibly made of sediments resulting from the

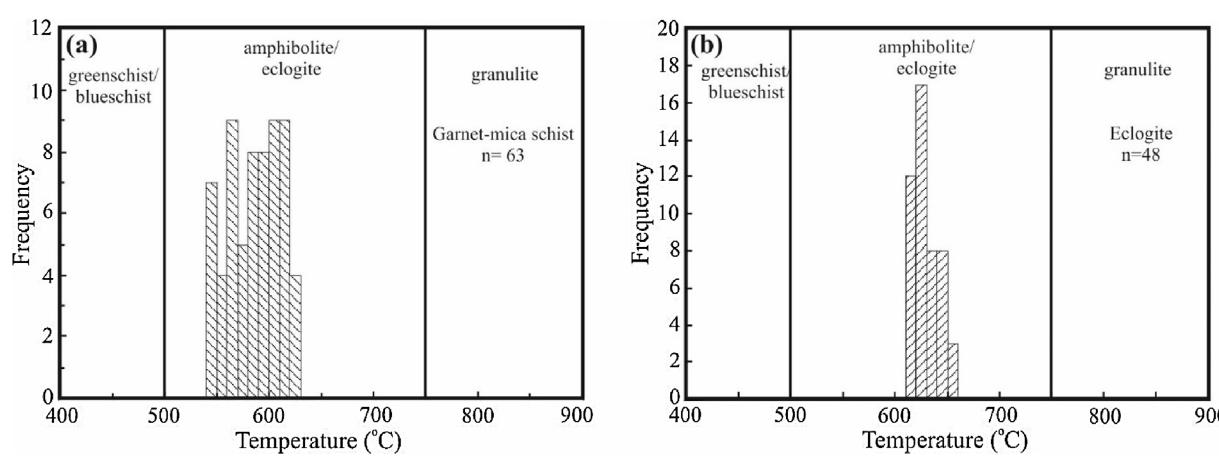

Fig. 9. (a, b) Frequency histograms of calculated formation temperatures for metapelitic and metamafic rutiles from garnet-mica schist and eclogite. Temperatures were calculated by using the Zr-in-rutile thermometer of Tomkins et al. (2007).

erosion of an old crustal or margin sediment. The eclogites represent a piece of a former oceanic crust with its associated sediments.

Rutile is principally formed during medium to high-grade metamorphism and not generally occurring in igneous and low-grade metamorphic rocks (Force, 1980). Thus, medium to high-grade metamorphic rocks can be considered to the main primary source of detrital rutile (Force, 1980). There is no input of metapelitic detrital rutile from greenschist- or blueschist-facies metamorphic rocks according to the calculated formation temperatures for metapelitic and metamafic rutiles (Fig. 9). The metapelitic rutiles are derived from amphibolite and eclogite-facies metamorphic rocks. Rb–Sr phengite ages from two eclogite samples in the Çetmi mélange gave a mid-Cretaceous age of ~100 Ma (Okay and Satır, 2000b). The upper time limit for deposition is set by mid-Cretaceous high-pressure metamorphism. The source rocks of detrital rutiles derived from amphibolite- and eclogite-facies rocks could be found in basement rocks of the Biga Peninsula (Kazdağ Massif), Balkan region (Rhodope Massif, Serbo-Macedonian Massif, Sredna Gora Zone) since amphibolite- and eclogite-facies rocks of pre-mid-Cretaceous age have been reported there (e.g., Okay et al., 1996; Reischmann and Kostopoulos, 2002; Carrigan et al., 2006; Gaggero et al., 2009; and references therein). Amphibolite-facies metamorphic basement rocks of the Kazdağ Massif located on the south of the Biga Peninsula are mainly composed of felsic gneisses, amphibolite, marble and meta-ophiolitic rocks at the basal – middle part of the massif, and metagranite associated migmatite, amphibolite, and marble intercalations at the top (e.g., Okay et al., 1991; Okay and Satır, 2000b; Duru et al., 2004; Erdoğan et al., 2013). Peak P-T conditions of amphibolite-facies rocks in the Kazdağ Massif are 5 ± 1 kbar and $640 \pm 50\,^{\circ}C$ (Okay and Satır, 2000b). Zircon ages from felsic gneisses and amphibolite in the Kazdağ Massif determined by single-zircon stepwise Pb evaporation method are 308 ± 16 Ma and 329 ± 5 Ma, respectively (Okay et al., 1996). The metamorphic rocks of the Kazdağ Massif underwent amphibolite-facies metamorphism under progressive compression during the Alpine orogeny, associated with the emplacement of metagranites (Okay and Satır, 2000b; Erdoğan et al., 2013). Metamorphism resulted from northward subduction of the İzmir-Ankara branch of the Neo-Tethyan Ocean under the Sakarya Zone. Following metamorphism, the medium to high-grade metamorphic rocks of the Kazdağ Massif were internally imbricated by southerly compression during collision. When evaluated from a tectonic point of view, the Kazdağ metamorphic sequence was imbricated along thrust faults of southward vergence after Alpine metamorphism (Erdoğan et al., 2013). Collision of the Sakarya Zone with the Anatolide-Tauride Block and internal imbrications of the Kazdağ Massif gave rise to progressive thickening in the crust. Amphibolite-facies rocks of the Kazdağ Massif could be the primary source rocks for the metapelitic detrital rutiles in the garnet-mica schist from the Çetmi mélange based on metamorphic conditions, geochemistry and tectonic setting. Amphibolite-facies rocks of the Kazdağ Massif could also be potential source rocks of the metamafic detrital rutiles. Metapelitic and metamafic detrital rutiles derived from amphibolite and eclogite-facies rocks may have transferred into the metasedimentary rocks in the Çetmi mélange before Cretaceous time. Another potential source for the detrital rutiles of the garnet-mica schist within the Çetmi mélange could be the Carboniferous flysch of the Istanbul Zone in Turkey. U-Pb rutile ages yielded Late Devonian-Early Carboniferous and their geochemistry show an amphibolite-facies metamorphic provenance dominated by metapelitic rocks (Okay et al., 2011). The calculated metamorphic temperatures of the metapelitic rutiles range between 550 and 750 °C (Okay et al., 2011).

Amphibolite to eclogite-facies metamorphic rocks have also been documented from the Rhodope and Serbo-Macedonian massifs of Bulgaria and Greece, and Sredna Gora Zone of Bulgaria. HP metamorphism with peak conditions of $585 \pm 32\,^{\circ}C$ and 2.17 ± 0.1 GPa in kyanite eclogite and $619 \pm 53\,^{\circ}C$ and 1.69 ± 0.17 GPa in common eclogite from the Kechros Complex in the eastern Rhodope (Mposkos et al., 2012). Moreover, HP/UHP metamorphism has been reported from the Kimi Complex, which has minimum temperature of 800 °C and pressure of 23 kbar (Bauer et al., 2007; Krenn et al., 2010). The timing of HP/UHP metamorphism in the Rhodope Massif is at 160 Ma (e.g., Mposkos and Krohe, 2006; Bauer et al., 2007). Moreover, the time of amphibolite-facies metamorphism is given as 144 Ma (Krenn et al., 2007). The estimated temperatures calculated by Thermocalc at 1.12–1.29 GPa are in the range of 602–661 °C for the eclogite-facies metabasites in the Sredna Gora Zone (Bulgaria) based on the assemblage garnet-clinopyroxene-amphibole-quartz and in the range of 569–665 °C temperature at 0.5 GPa for the amphibolite-facies assemblage of biotite-muscovite-plagioclase-quartz (Gaggero et al., 2009). Eclogite-bearing amphibolites yielded 398.4 ± 5.2 Ma (Ar–Ar dating on hornblende, Gaggero et al., 2009).

7. Conclusions

The following major conclusions are derived from this study of high-pressure metamorphic rocks in the Biga Peninsula:

1) 85% of the detrital rutile grains from garnet-mica schist were derived from metapelitic and 15% from metamafic rocks based on the Cr-Nb discrimination diagram. Composition and temperature range of Zr-in-rutile grains from garnet-mica schist suggest that metapelitic rutiles accurately reflect their provenance. On the other hand, eclogites in the Çetmi mélange have typical compositions for derivation from metamafic rocks.
2) The rutile grains in garnet-mica schist are mostly characterized by subchondritic Nb/Ta ratios (7–24) with an average of 15. The Nb/Ta and Zr/Hf ratios of rutiles in eclogite samples increase with a decrease in Ta and Hf contents, which could be ascribed to the effect of metamorphic dehydration in subduction zones on rutile Nb/Ta differentiation. The rutile grains are dominated by subchondritic Nb/Ta and Zr/Hf ratios. It can be noted that the subchondritic Nb/Ta ratios may record rutile growth from local sinks of aqueous fluids from metamorphic dehydration. Subchondritic Nb/Ta ratios of rutile would be produced if their growth is associated with prograde eclogite-facies metamorphism during subduction.
3) The calculated formation temperatures of high-pressure metasedimentary rocks vary from 540 °C to 624 °C with an average of 586 °C at P = 2.3 GPa. The calculated Zr-in-rutile temperatures for the garnet-mica schist demonstrate that there is no derivation of metapelitic rutiles from blueschist- to greenschist-facies rocks. Amphibolite to eclogite-facies rocks are the most convenient candidates for this type of detrital rutile. The Zr-in-rutile thermometer of Tomkins et al. (2007) gives temperatures of 611–659 °C with an average temperature of 630 °C for eclogites from the Çetmi mélange. This average temperature suggests the growth temperature of rutile. It can be noted that both Zr contents and calculated temperatures of inclusion rutiles and matrix rutiles from eclogite samples overlap to each other. This suggests that all rutiles grew under the same P-T conditions during the subduction.
4) Amphibolite-facies rocks exposed on the Kazdağ Massif located in southern part of the Biga Peninsula could be the primary source rocks for the metapelitic detrital rutiles in the garnet-mica schist from the Çetmi mélange. Metamafic rocks that underwent the amphibolite-facies metamorphism in the Kazdağ Massif could be potential source rocks of the metamafic detrital rutiles. Metapelitic and metamafic rutiles derived

from amphibolite-facies rocks may have transferred into the metasedimentary rocks in the Çetmi mélange before mid-Cretaceous time.

Acknowledgments

This study was supported by the Scientific and Technological Research Council of Turkey (TÜBİTAK/114Y834) and Çanakkale Onsekiz Mart University Scientific Research Coordination Unit (grant number FBA-702-2016). Horst Marschall and Guido Meinhold are acknowledged for their constructive reviews and comments, which significantly helped to modify the manuscript. We thank A. Holzheid for careful editorial handling.

Appendix A. Supplementary data

Supplementary data associated with this article can be found, in the online version, at http://dx.doi.org/10.1016/j.chemer.2017.07.001.

References

Aygül, M., Topuz, G., Okay, A.I., Satır, M., Meyer, H.P., 2012. The kemer metamorphic complex (NW Turkey), a subducted continental margin of the sakarya zone. Turk. J. Earth Sci. 21, 19–35.
Barth, M.G., McDonough, W.F., Rudnick, R.L., 2000. Tracking the budget of Nb and Ta in the continental crust. Chem. Geol. 165, 197–213.
Bauer, C., Rubatto, D., Krenn, K., Proyer, A., Hoinkes, G., 2007. A zircon study from the Rhodope metamorphic complex, N-Greece: time record of a multistage evolution. Lithos 99, 207–228.
Beccaletto, L., Jenny, C., 2004. Geology and correlation of the ezine zone: a rhodope fragment in NW Turkey? Turk. J. Earth Sci. 13, 145–176.
Beccaletto, L., Bartolini, A.C., Martini, R., Hochuli, P.A., Kozur, H., 2005. Biostratigraphic data from Çetmi melange, northwest Turkey: palaeogeographic and tectonic implications. Palaeogeogr. Palaeoecl. 221, 215–244.
Beccaletto, L., Bonev, N., Bosch, D., Bruguier, O., 2007. Record of a palaeogene syn-collisional extension in the north aegean sea: evidence from the kemer micaschists (NW Turkey). Geol. Mag. 144, 393–400.
Beccaletto, L., 2004. Geology, Correlations and Geodynamic Evolution of the Biga Peninsula, Northwest Turkey (PhD Thesis). University of Lausanne, Switzerland, pp. 1–146.
Brenan, J.M., Shaw, H.F., Phinney, D.L., Ryerson, F.J., 1994. Rutile-aqueous fluid partitioning of Nb, Ta, Hf, Zr, U and Th: implications for high field strength element depletions in island-arc basalts. Earth Planet. Sci. Lett. 128, 327–339.
Carrigan, C.W., Mukasa, S.B., Haydoutov, I., Kolcheva, K., 2006. Neoproterozoic magmatism and Carboniferous high-grade metamorphism in the Sredna Gora Zone: an extension of the Gondwana-derived Avalonian-Cadomian belt? Precambrian Res. 147, 404–416.
Cavazza, W., Okay, A.I., Zattin, M., 2009. Rapid early-middle exhumation of the kazdağ massif (western anatolia). Int. J. Earth Sci. 98, 1935–1947.
Chen, Z.Y., Li, Q.L., 2008. Zr-in-rutile thermometry in eclogite at Jinheqiao in the Dabie orogen and its geochemical implications. Chin. Sci. Bull. 53, 768–776.
Cherniak, D.J., Mancheste, J., Watson, E.B., 2007. Zr and Hf diffusion in rutile. Earth Planet. Sci. Lett. 261, 267–279.
Ding, X., Lundstrom, C., Huang, F., Li, J., Zhang, Z.M., Sun, X.M., Liang, J.L., Sun, W.D., 2009. Natural and experimental constraints on formation of the continental crust based on niobium-tantalum fractionation. Int. Geol. Rev. 51, 473–501.
Ding, X., Hu, Y.H., Zhang, H., Li, C.Y., Ling, M.X., Sun, W.D., 2013. Major Nb/Ta fractionation recorded in garnet amphibolite facies metagabbro. J. Geol. 121, 255–274.
Duru, M., Pehlivan, Ş., Şentürk, Y., Yavaş, F., Kar, H., 2004. New results on the lithostratigraphy of the kazdağ massif in northwest Turkey. Turk. J. Earth Sci. 13, 177–186.
Eggins, S., Kinsley, L., Shelley, J., 1998. Deposition and element fractionation processes during atmospheric pressure laser sampling for analysis by ICP-MS. Appl. Surf. Sci. 127-129, 278–286.
Erdoğan, B., Akay, E., Hasözbek, A., Satır, M., Siebel, W., 2013. Stratigraphy and tectonic evolution of the Kazdağ Masif (NW Anatolia) based on field studies and radiometric ages. Int. Geol. Rev. 55 (16), 2060–2082.
Ewing, T.A., Herman, J., Rubatto, D., 2013. The robustness of the Zr-in-rutile and Ti-in-zircon thermometers during high-temperature metamorphism (Ivrea-Verbano zone, northern Italy). Contrib. Mineral. Petrol. 165, 757–779.
Foley, S.F., Barth, M.G., Jenner, G.A., 2000. Rutile/melt partition coefficients for trace elements and assessment of the influence of rutile on the trace element characteristics of subduction zone magmas. Geochim. Cosmochim. Acta 64, 933–938.
Force, E.R., 1980. The provenance of rutile. J. Sediment. Petrol. 50 (2), 485–488.
Gaggero, L., Buzzi, L., Haydoutov, I., Cortesogno, L., 2009. Eclogite relics in the Variscan orogenic belt of Bulgaria (SE Europe). Int. J. Earth. Sci. 98, 1853–1877.
Gao, X.Y., Zheng, F.Y., Xia, X.P., Chen, Y.P., 2014. U-Pb ages and trace element of metamorphic rutile from ultrahigh-pressure quartzite in the Sulu orogen. Geochim. Cosmochim. Acta 143, 87–114.
Green, T.H., 1995. Significance of Nb/Ta as an indicator of geochemical processes in the crust?mantle system. Chem. Geol. 120, 347–359.
Hermann, J., Spandler, C., Hack, A., Korsakov, A., 2006. Aqueous fluids and hydrous melts in high-pressure and ultra-high pressure rocks: implications for element transfer in subduction zones. Lithos 92, 399–417.
Huang, J., Xiao, Y.L., Gao, Y.J., Hou, Z.H., Wu, W., 2012. Nb-Ta fractionation induced by fluid-rock interaction in subduction-zones: constraints from UHP eclogite- and vein-hosted rutile from the Dabie orogen, Central-Eastern China. J. Metamor. Geol. 30, 821–842.
Jochum, K.P., Nehring, F., 2006. NIST 610: GeoReM preferred values (11/2006). GeoReM http://georem.mpch-mainz.gwdg.de.
John, T., Klemd, R., Klemme, S., Pfander, J., Hoffmann, J., Gao, J., 2011. Nb?Ta fractionation by partial melting at the titanite?rutile transition. Contrib. Mineral Petrol. 161, 35–45.
Klemme, S., Prowatke, S., Hametner, K., Günther, D., 2005. Partitioning of trace elements between rutile and silicate melts: implications for subduction zones. Geochim. Cosmochim. Acta 69, 2361–2371.
Krenn, K., Bauer, C., Proyer, A., Hoinkes, G., 2007. Geodynamic Evolution of an UHP Suture Zone in the Greek Rhodope. American Geophysical Union (Fall Meeting, abstract V13A-1137).
Krenn, K., Bauer, C., Proyer, A., Klötzli, U., Hoinkes, G., 2010. Tectonometamorphic evolution of the Rhodope orogen. Tectonics 29 (4), 1–25.
Liu, L., Xiao, Y., Wörner, G., Kronz, A., Simon, K., Hou, Z., 2014. Detrital rutile geochemistry and thermometry from the Dabie orogen: implications for source–sediment links in a UHPM terrane. J. Afr. Earth Sci. 89, 123–140.
Luvizotto, G.L., Zack, T., Meyer, H.P., Ludwig, T., Triebold, S., Kronz, A., Münker, C., Stockli, D.F., Prowatke, S., Klemme, S., Jacop, D.E., von Eynatten, H., 2009. Rutile crystals as potential trace element and isotope mineral standards for microanalysis. Chem. Geol. 261, 346–369.
Münker, C., Pfänder, J.A., Weyer, S., Büchl, A., Kleine, T., Mezger, K., 2003. Evolution of planetary cores and the Earth?Moon system from Nb/Ta systematic. Science 301, 84–87.
Münker, C., 1998. Nb/Ta fractionation in a Cambrian arc back arc system, New Zealand: source constraints and application of refined ICPMS techniques. Chem. Geol. 144, 23–45.
M.T.A, 2012. General and economic geology of the Biga Peninsula. Special Publication Series, vol. 28, 326 p. (in Turkish).
Meinhold, G., Anders, B., Kostopoulos, D., Reischmann, T., 2008. Rutile chemistry and thermometry as provenance indicator: an example from Chios Island, Greece. Sediment. Geol. 203 (1–2), 98–111.
Meinhold, G., Kostopoulos, D., Frei, D., Himmerkus, F., Reischmann, T., 2010. U-Pb LA-SF-ICP-MS zircon geochronology of the serbo-Macedonian massif, Greece: palaeotectonic constraints for gondwana-derived terranes in the eastern mediterranean. Int. J. Earth Sci. 99, 813–832.
Meinhold, G., 2010. Rutile and its applications in earth sciences. Earth Sci. Rev. 102, 1–28.
Meyer, M., John, T., Brandt, S., Klemd, R., 2011. Trace element composition of rutile and the application of Zr-in-rutile thermometry to UHT metamorphism (Epupa Complex, NW Namibia). Lithos 126, 388–401.
Morton, A.C., Chenery, S., 2009. Detrital rutile geochemistry and thermometry as guides to provenance of Jurassic-Paleocene sandstones of the Norwegian Sea. J. Sediment. Res. 79 (7–8), 540–553.
Morton, A.C., Hallsworth, C.R., 1999. Processes controlling the composition of heavy mineral assemblages in sandstones. Sediment. Geol. 124 (1–4), 3–29.
Mposkos, E., Krohe, A., 2006. Pressure-temperature-deformation paths of closely associated ultra-high pressure (diamond-bearing) crustal and mantle rocks of the Kimi Complex: implications for the tectonic history of the Rhodope Mountains northern Greece. Can. J. Earth Sci. 43, 1755–1776.
Mposkos, E., Baziotis, I., Proyer, A., 2012. Pressure-temperature evolution of eclogites from the Kechros complex in the Eastern Rhodope (NE Greece). Int. J. Earth Sci. 101, 973–996.
Nichols, G.T., Wyllie, P.J., Stern, C.R., 1994. Subduction zone-melting of pelagic sediments constrained by melting experiments. Nature 371 (6500), 785–788.
Okay, A.İ., Göncüoğlu, M.C., 2004. The karakaya complex: a review of data and concepts. Turk. J. Earth Sci. 13, 77–95.
Okay, A.I., Satır, M., 2000a. Upper cretaceous eclogite-facies metamorphic rocks from the biga peninsula, northwest Turkey. Turk. J. Earth Sci. 9, 47–56.
Okay, A.İ., Satır, M., 2000b. Coeval plutonism and metamorphism in a latest Oligocene metamorphic core complex in Northwest Turkey. Geol. Mag. 137, 495–516.
Okay, A.I., Siyako, M., Bürkan, K.A., 1990. Geology and tectonic evolution of the Biga Peninsula. Turk. Assoc. Petrol. Geol. Bull. 2/1, 83–121.
Okay, A.İ., Siyako, M., Bürkan, K.A., 1991. Geology and tectonic evolution of the Biga Peninsula. In: Dewey, J.F. (Ed.), Special Issue on Tectonics. Bull Tech. Univ. Ist. (44, pp. 191–255).
Okay, A.I., Satır, M., Maluski, H., Siyako, M., Monie, P., Metzger, R., Akyüz, S., 1996. Paleo- and Neotethyan events in northwest Turkey. In: Yin, A., Harrison, M. (Eds.), Tectonics of Asia. Cambridge University Press, Cambridge, pp. 420–441.
Okay, A.İ., Satir, M., Siebel, W., 2006. Pre-Alpide and Mesozoic orogenic events in the Eastern Mediterranean region. In: Gee, D., Stephenson, R. (Eds.), European

Lithosphere Dynamics, vol. 32. Geological Society London, Memoir, pp. 389–405.

Okay, N., Zack, T., Okay, A.I., Barth, M., 2011. Sinistral transport along the Trans-European Suture Zone: detrital zircon–rutile geochronology and sandstone petrography from the Carboniferous flysch of the Pontides. Geol. Mag. 148 (3), 380–403.

Reischmann, T., Kostopoulos, D., 2002. Timing of UHPM in metasediments from the rhodope massif, N. Greece. In: Proceedings Goldschmidt Conf., Davos, Switzerland, p. 634.

Rudnick, R.L., Barth, M., Horn, I., McDonough, W.F., 2000. Rutile-bearing refractory eclogites: missing link between continents and depleted mantle. Science 287, 278–281.

Saunders, A., Tarney, J., Weaver, S., 1980. Traverse geochemical variations across the Antarctic Peninsula: implications for the genesis of calc-alkaline magmas. Earth Planet. Sci. Lett. 46, 344–360.

Schmidt, M.W., Dardon, A., Chazot, G., Vannucci, R., 2004. The dependence of Nb and Ta rutile–melt partitioning on melt composition and Nb/Ta fractionation during subduction processes. Earth Planet. Sci. Lett. 226, 415–432.

Schmidt, A., Weyer, S., Mezger, K., Scherer, E.E., Xiao, Y.L., Hoefs, J., Brey, G.P., 2008. Rapid eclogitisation of the Dabie-Sulu UHP terrane: constraints from Lu?Hf garnet geochronology. Earth Planet. Sci. Lett. 273, 203–213.

Schmidt, A., Weyer, S., John, T., Brey, G.P., 2009. HFSE systematics of rutile-bearing eclogites: new insights into subduction zone processes and implications for the earth's HFSE budget. Geochim. Cosmochim. Acta 73, 455–468.

Spear, F.S., Wark, D.A., Cheney, J.T., 2006. Zr-in-rutile thermometry in blueschists from Sifnos, Greece. Contrib. Mineral. Petrol. 152, 375–385.

Stendal, H., Toteu, S.F., Frei, R., Penaye, J., Nje, L., Bassahak, J., Nni, J., Kankeu, B., Ngako, V., Hell, J.V., 2006. Derivation of detrital rutile in the Yaounde region from the Neoproterozoic Pan-African belt in southern Cameroon (Central Africa). J. Afr. Earth Sci. 44 (4–5), 443–458.

Şengün, F., Zack, T., 2016a. Trace element composition of rutile and Zr-in-rutile thermometry in meta-ophiolitic rocks from the Kazdağ Massif, NW Turkey. Mineral. Petrol. 110, 547–560.

Şengün, F., Zack, T., 2016b. Application of the titanium-in-quartz thermobarometer to eclogites from the Biga Peninsula NW Turkey. WMESS 2016, IOP Conference Series: Earth and Environmental Science vol. 44, 1–6.

Şengün, F., Yigitbas, E., Tunç, İ.O., 2011. Geology and tectonic emplacement of eclogite and blueschist biga peninsula, northwest Turkey. Turk. J. Earth Sci. 20, 273–285.

Şengün, F., Davis, P.B., Tunç İ, O., Yigitbas, E., 2012. Petrology and geochemistry of eclogites from the Biga Peninsula, Northwest Turkey. Geodin. Acta 25 (3-4), 248–266.

Tomkins, H.S., Powell, R., Ellis, D.J., 2007. The pressure dependence of the zirconium-in-rutile thermometer. J. Metamorph. Geol. 25, 703–713.

Triebold, S., von Eynatten, H., Luvizotto, G.L., Zack, T., 2007. Deducing source rock lithology from detrital rutile geochemistry An example from the Erzgebirge. Germany.Chem. Geol. 244, 421–436.

Tunç, İ.O., 2008. Geology of the Kazdağ Massif Rocks on the Southern of Bayramiç (Çanakkale) Master Thesis. Çanakkale Onsekiz Mart University, Çanakkale, Turkey.

Van Achterbergh, E., Ryan, C.G., Griffin, W.L., 2000. GLITTER (Version 3.0, On-line Interactive Data Reduction for LA-ICPMS). Maquarie Research Ltd.

Watson, E.B., Wark, D.A., Thomas, J.B., 2006. Crystallization thermometers for zircon and rutile. Contrib. Mineral. Petrol. 151, 413–433.

Xiao, Y.L., Sun, W.D., Hoefs, J., Simon, K., Zhang, Z.M., Li, S.G., Hofmann, A.W., 2006. Making continental crust through slab melting: constraints from niobium/tantalum fractionation in UHP metamorphic rutile. Geochim. Cosmochim. Acta 70, 4770–4782.

Yaltırak, C., Okay, A.I., 2004. Geology of the Palaeo-Tethyan Units on the northern of Edremit Bay. Bull. Engin. ITU 3, 67–79.

Zack, T., Kronz, A., Foley, S.F., Rivers, T., 2002. Trace element abundances in rutiles from eclogites and associated garnet mica schists. Chem. Geol. 184, 97–122.

Zack, T., Moraes, R., Kronz, A., 2004. Temperature dependence of Zr in rutile: empirical calibration of a rutile thermometer. Contrib. Mineral. Petrol. 148, 471–488.

Zheng, Y.F., Xia, Q.X., Chen, R.X., Gao, X.Y., 2011. Partial melting, fluid supercriticality and element mobility in ultrahigh-pressure metamorphic rocks during continental collision. Earth Sci. Rev. 107, 342–374.